Journal of Photochemistry and Photobiology A: Chemistry 346 (2017) 452–461

Contents lists available at ScienceDirect

Journal of Photochemistry and Photobiology A: Chemistry

journal homepage: www.elsevier.com/locate/jphotochem

Photodynamic properties and photoinactivation of microorganisms mediated by 5,10,15,20-tetrakis(4-carboxyphenyl)porphyrin covalently linked to silica-coated magnetite nanoparticles

Ana C. Scanone, Natalia S. Gsponer, M. Gabriela Alvarez, Edgardo N. Durantini*

Departamento de Química, Facultad de Ciencias Exactas, Físico-Químicas y Naturales, Universidad Nacional de Río Cuarto, Ruta Nacional 36 Km 601, X5804BYA Río Cuarto, Córdoba, Argentina

ARTICLE INFO

Article history:
Received 3 February 2017
Received in revised form 20 June 2017
Accepted 25 June 2017
Available online 27 June 2017

Keywords:
Porphyrin
Magnetic nanoparticles
Photosensitizer
Photooxidation
Singlet oxygen
Photodynamic inactivation

ABSTRACT

Magnetic nanoparticles of Fe_3O_4 (MNP) were synthesized by co-precipitating Fe^{2+} and Fe^{3+} ions in an ammonia solution. This MNP was coated with silica using sodium metasilicate to obtain silica-coated MNP (MNPSi). Grafting of aminopropyl groups on MNP or MNPSi was performed with (3-aminopropyl) trimethoxysilane to form $MNPNH_2$ or $MNPSiNH_2$, respectively. 5,10,15,20-Tetrakis(4-carboxyphenyl) porphyrin (TCPP) was covalently bound onto the $MNPNH_2$ or $MNPSiNH_2$ via carbodiimide activation to obtain MNPNH-TPCC or MNPNH-TPCC, respectively. These MNP presented an average diameter of about 15 nm. UV–vis absorption spectra presented the characteristic Soret and Q bands of TCPP covalently linked to the nanoparticles. The MNP containing TCPP produced a high photodecomposition of 2,2-(anthracene-9,10-diyl)bis(methylmalonate), which was used to detect singlet molecular oxygen $O_2(^1\Delta_g)$ production in water. Moreover, these nanoparticles sensitized the photooxidation of L-tryptophan in water, mainly mediated by a type II photoprocess. Photoinactivation of microorganisms was investigated in *Staphylococcus aureus*, *Escherichia coli* and *Candida albicans*. *In vitro* experiments showed that photosensitized inactivation induced by MNPSiNH-TCPP improved with an increase of irradiation times. After 30 min irradiation, a 2.5 log reduction was found for *S. aureus* and *C. albicans*. Also, the last conditions produced a decrease of 3 log in *E. coli*. Similar result was obtained MNPNH-TCPP. However, the main difference between these nanoparticles as photosensitizer was found after recycling experiments. While the photoinactivation mediated by MNPNH-TCPP rapidly decrease after one cycle, MNPSiNH-TCPP was still efficient after three cycles of inactivation. Therefore, MNPSiNH-TCPP is an interesting and versatile photodynamic active material to eradicate microorganisms.

1. Introduction

Infectious diseases may become non curable owing to high levels of multiple drug resistant pathogens [1]. The best epidemiologically documented resistance with high clinical impact includes the Gram-positive pathogen *Staphylococcus aureus* [2]. In this context, the Gram-negative organism *Escherichia coli*, not only causes severe hospital-acquired infections but also has an important reservoir in animals and the environment. Moreover, the clinical outcome of a systemic fungal infection is a very difficult task and the antifungal drug resistance is one of factors contributing to therapeutic failure [3]. In particular, antifungal drug resistance is just one of many factors contributing to therapeutic failure in *Candida albicans*. Therefore, microbial resistance against antibiotics is a serious global health issue and it has posed new challenge to researchers [1]. Photodynamic inactivation (PDI) has been proposed as an interesting approach to eradication of microorganisms [4]. In general, PDI involves the addition of a photosensitizer that is rapidly bound to cells. The irradiation of the infection with visible light in presence of oxygen produces highly reactive oxygen species (ROS). In PDI, two mechanisms can be mainly involved after activation of the photosensitizer [5]. In the type I pathway, the photosensitizer can interacts with different substrates to form free radicals. These radicals can also interact with oxygen producing ROS. In the type II partway, the photosensitizer generates singlet molecular oxygen, $O_2(^1\Delta_g)$, by energy transfer [6]. Thus, the ROS react with biomolecules of cellular environment. These processes induce a loss of biological functionality leading to cell inactivation [7].

* Corresponding author.
E-mail address: edurantini@exa.unrc.edu.ar (E.N. Durantini).

http://dx.doi.org/10.1016/j.jphotochem.2017.06.039
1010-6030/

Most of PDI investigations have been carried out adding the photosensitizer to cell suspensions. In this approach, after treatment traces of the photosensitizer can remain in the medium. These molecules can produce an undesired remnant photodynamic effect. This inconvenient can be avoided using a light-activated antimicrobial photosensitizer linked to supports [8]. Thus, the concept of using photosensitizers immobilized on a surface for this purpose is intended to address a range of economic, ecological and public health issues. These materials kill microbes by the action of light and have potential applications in domestic and healthcare settings [9]. Therefore, the development of techniques that can selectively deliver drugs to the pathological sites is currently one of the most important areas of drug research [10]. The emergence of nanotechnology is likely to have a significant impact on the drug-delivery sector. Nanoparticles are at the leading edge, with many potential applications in clinical medicine. Magnetic nanoparticles (MNP) can be used to immobilize photosensitizers, taking into account the possibility of recovery and reuse. Superparamagnetic iron oxide nanoparticles with appropriate surface chemistry have been considered for numerous *in vivo* applications [11]. The use of MNP for the dispersion of a photosensitizer can facilitate the recovery from the environment by applying a magnetic field. In this sense, silica based nanomagneto-porphyrin hybrids were particularly interesting due to the possibility of being purified and isolated through a magnetic field. Thus, nanomagnet-porphyrin hybrids have been studied as efficient photosensitizers for the photoinactivation of bacteria and phages [12,13].

In the present study, 5,10,15,20-tetrakis(4-carboxyphenyl) porphyrin (TCPP) was attached to MNP of Fe_3O_4 without a shell of silica and coated with silica (MNPSi) through amide bonds to obtain MNPNH-TCPP and MNPSiNH-TCPP, respectively (Scheme 1). The spectroscopic and photodynamic properties of these MNPs were compared in water using different photooxidizable substrates. Moreover, photodynamic action of the resultant modified MNP was investigated *in vitro* to inactivate a Gram-positive, *Staphylococcus aureus* and a Gram-negative, *Escherichia coli* bacteria and a yeast, *Candida albicans*. These investigations were also focused on the ability to recycle these MNP

2. Materials and methods

2.1. General

Transmission electron microscopy (TEM) images were recorded on a Hitachi H-7500 microscope (Tokyo, Japan) operated at 120 kV. Magnetic decantation was performed using a neodymium magnet (20 mm diameter × 10 mm thick). Absorption spectra were carried out on a Shimadzu UV-2401PC spectrometer (Shimadzu Corporation, Tokyo, Japan), using a quartz cell of 1 cm path length. FT-IR spectra were recorded on a Bruker Tensor 27 (Ettlingen, Germany). Cell growth was measured with a Turner SP-830 spectrophotometer (Dubuque, IA, USA). Fluence rates were obtained with a Radiometer Laser Mate-Q (Coherent, Santa Clara, CA, USA). Photooxidation of substrates were carried out with a Cole-Parmer

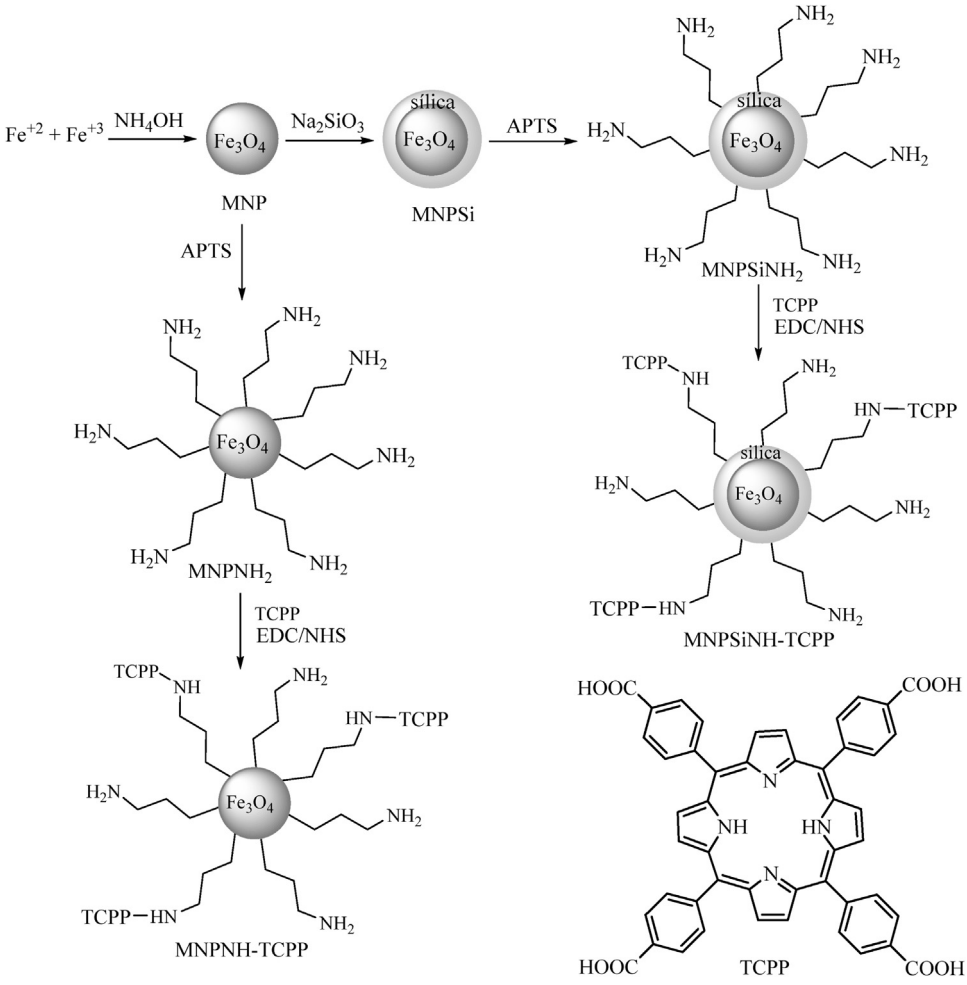

Scheme 1. Synthesis procedure of MNPNH-TAPP and MNPSiNH-TAPP.

illuminator 41720-series (Cole-Parmer, Vernon Hills, IL, USA) with a 150 W halogen lamp through a high intensity grating monochromator (Photon Technology Instrument, Birmingham, NJ, USA). Optical filters (GG455 cutoff filter) were used to select a wavelength range between 455 and 800 nm (44 mW/cm^2). The visible light source used to irradiate cell suspensions was a Novamat 130 AF (Braun Photo Technik, Nürnberg, Germany) slide projector containing with a 150 W lamp. A 2.5 cm glass cuvette filled with water without circulation was used to remove the heat from the lamp. The temperature was remained below 30 °C during the experiments as monitored with an electronic digital thermometer with stainless steel probe (Digi-thermo, Sigma, St. Louis, MO, USA). A wavelength range between 350 and 800 nm was selected by optical filters with a fluence rate of 90 mW/cm^2. Cell suspensions in 96-well microtiter plates were irradiated from above at a distance of 2 cm.

Chemicals from Aldrich (Milwaukee, WI, USA) were used without further purification. 5,10,15,20-Tetrakis(4-carboxyphenyl) porphyrin (TCPP) and 5,10,15,20-tetra(4-sulphonatophenyl)porphyrin ($TPPS^{4-}$) sodium salt were purchased from Aldrich. Tetrasodium 2,2′-(anthracene-9,10-diyl)bis(methylmalonate) (ABMM) was prepared as previously described [14]. Phosphate-buffered saline (PBS) solution of 10 mM pH = 7.0 was used. Solvents (GR grade) from Merck (Darmstadt, Germany) were distilled. Ultrapure water was obtained from a Labconco (Kansas, MO, USA) equipment model 90901-01.

2.2. Synthesis of MNP derivatives

The Fe_3O_4 core was obtained by the conventional coprecipitation method with some modifications (Scheme 1) [12]. Thus, $FeCl_2{\cdot}4H_2O$ (0.55 g, 2.7 mmol) and $FeCl_3{\cdot}6H_2O$ (1.50 g, 5.5 mmol) were dissolved in 1.5 mL water with vigorous stirring under an argon atmosphere. The mixture was heated at 80 °C and NH_4OH (1.75 mL, 25% v/v) was added dropwise to the solution. The color of the bulk solution immediately changed from orange to black. A pH = 9 was verified and the mixture was allowed to react for 30 min at 80 °C, with continuous stirring under argon atmosphere. The magnetite was separated by magnetic decantation and several washes were carried out with water. Then, nanoparticles were resuspended in 20 mL water and centrifuged (16,000 rpm, 5 min) to remove the aggregated nanoparticles. After that the supernatant was separated, nanoparticles were magnetically decanted and resuspended in 5 mL water to obtain a stock suspension of ~100 mg MNP/mL.

A solution of sodium metasilicate (0.9 M) was prepared in water. The pH value of the solution was adjusted to 12 by the addition of a required amount of concentrated hydrochloric acid (37%). The sodium metasilicate solution and the prepared Fe_3O_4 nanocores (~50 mg MNP/mL) were ultrasonicated for 30 min. Then, the temperature of the mixture was increased to 80 °C. The mixture was allowed to reach room temperature and hydrochloric acid was added dropwise to adjust the pH value to 6–7 [12]. Nanoparticles were magnetically decanted and washed several times with water to obtain a stock solution of ~60 mg MNPSi/mL.

MNPSi were washed with acetone by magnetic decantation, resuspended in 4 mL acetone and sonicated for 45 min. Then, a solution of (3-aminopropyl)triethoxysilane (APTS) in toluene (0.3 M) was added [15]. Excessive APTS was added to obtain APTS-coated nanoparticles [16]. The mixture was heated at 60 °C for 4 h and kept at 37 °C for 12 h with continuous stirring under argon atmosphere. Nanoparticles were magnetically decanted and washed with toluene and ethanol. Then, nanoparticles were dispersed in 5 mL water to yield a stock suspension of ~50 mg $MNPSiNH_2$/mL. In the same way, MNP were treated with APTS to obtain a stock suspension of ~50 mg $MNPNH_2$/mL. IR spectra of $MNPSiNH_2$ and $MNPSiNH_2$ agree with those previously reported [16,17].

A solution of *N*-hydroxysuccinimide (NHS, 20 μmol in 1.5 mL PBS) and 1-ethyl-3-(3-dimethylaminopropyl)carbodiimide hydrochloride (EDC, 20 μmol in 1.5 mL PBS) was added dropwise to the solution of TCPP (5 μmol) in 1 mL *N*,*N*-dimethylformamide (DMF). The mixture was stirred for 2 h at 25 °C to activate TCPP [18]. After that, 15 mg $MNPSiNH_2$ was added to the solution of TCPP/EDC/NHS and the mixture was stirred for 24 h at 25 °C under argon atmosphere. Then, nanoparticles were washed several times with ethanol and water to eliminate the excess of TCPP. MNPSiNH-TCPP were resuspended in 5 mL water obtaining a stock suspension of ~3 mg MNPSiNH-TCPP/mL. Similar approach was used with $MNPNH_2$ to produce a suspension of ~3 mg MNPNH-TCPP/mL. Stock suspension of 3 mg nanoparticles/mL, containing 3.0 nmol TCPP/mg nanoparticles, were prepared in water, which represents 9.0 μM TCPP.

2.3. Determination of the amount of TCPP covalently bound to nanoparticles

A solution of 1-fluoro-2,4-dinitrobenzene (FDNB, 5.0×10^{-4} M, 2 mL) in THF was stirred with different stock suspensions of nanoparticles: a) MNPSi (70 mg), b) $MNPSiNH_2$ (70 mg) and c) MNPSiNH-TCPP (70 mg) at room temperature for 6 h [19]. The excess of FDNB was separated from nanoparticles by magnetic decantation and the supernatant was reacted with *n*-butylamine (10.1 M, 10 μL, final concentration 5.0×10^{-2} M) to obtain *N*-butyl-2,4-dinitroaniline (BDNA) [20]. This product is yellow with a UV–visible absorption band at λ_{max} = 350 nm (ε = 5500 cm^{-1} M^{-1}). Absorptions of the samples were determined using aliquots of 200 μL in 2 mL of THF. Similar procedure was used with a) MNP

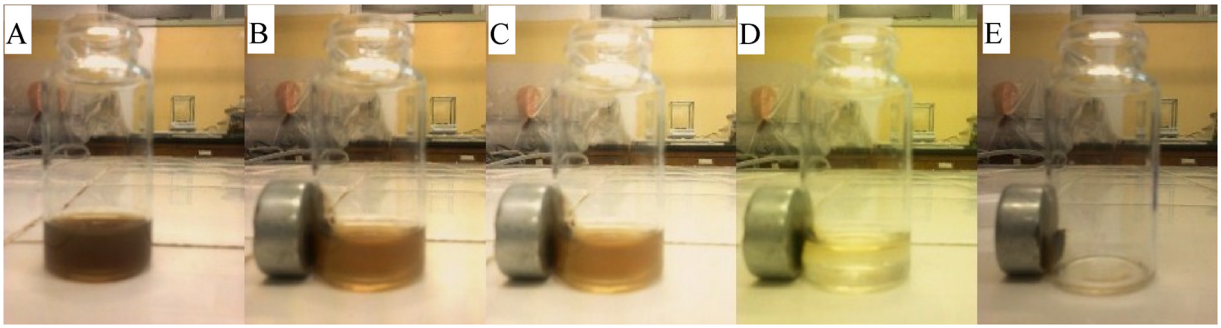

Fig. 1. Magnetic decantation washing sequence of $MNPSiNH_2$-TCPP with neodymium magnet 20 mm diameter × 10 mm thick, (A) water suspensions in the absence of a magnetic field, (B) 15 s, (C) 30 s and (D) 120 s after placing the magnet, (E) without the supernatant.

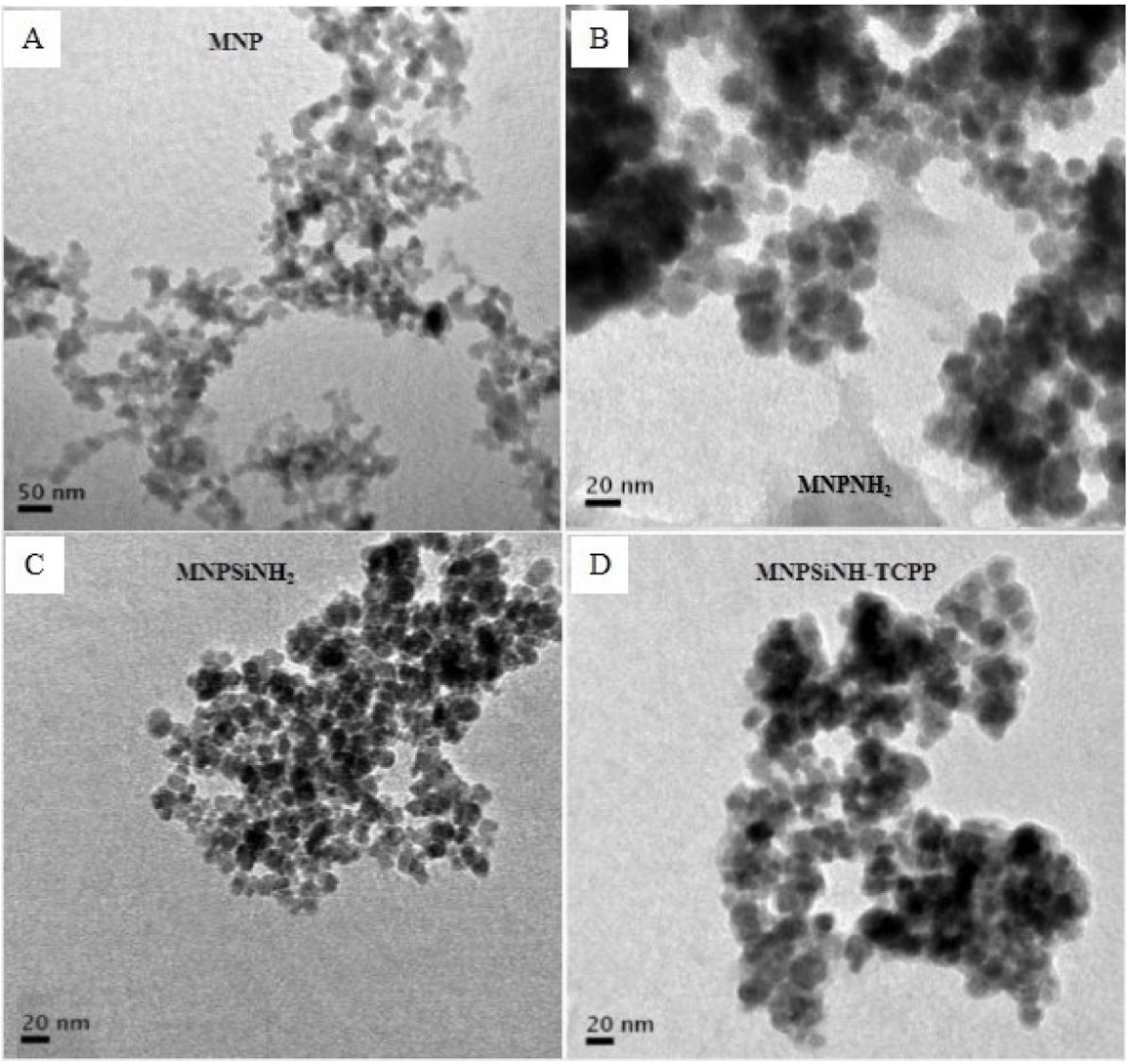

Fig. 2. Typical TEM images of (A) MNP, (B) $MNPNH_2$, (C) $MNPSiNH_2$ and (D) MNPSiNH-TCPP, showing that the particle size is around 15 nm.

(70 mg), b) $MNPNH_2$ (70 mg) and c) MNPNH-TCPP (70 mg). Also, the reaction between FDNB and *n*-Bu was performed in absence of MNPs under the same experimental condition.

2.4. Steady state photolysis

Solutions of ABMM (35 μM) and photosensitizer (3 μM) in water (2 mL) were irradiated in 1 cm path length quartz cells. The photooxidation rate of ABMM were studied by following the decrease of the absorbance (A) at λ_{max} = 379 nm. The absorbance of the photosensitizers was normalized to 0.1 at 515 nm. The observed rate constants (k_{obs}) were determined by a linear least-squares fit of the semilogarithmic plot of Ln A_0/A *vs.* time. Quantum yields of $O_2(^1\Delta_g)$ production (Φ_Δ) were calculated comparing the k_{obs} for the corresponding photosensitizer with that for $TPPS^{4-}$, which was used as a reference (Φ_Δ = 0.71) [21]. Determinations of k_{obs} values for the sample and reference under the same conditions afforded Φ_Δ by direct comparison of the slopes in the linear region of the plots.

Solutions of L-tryptophan (Trp, 20 μM) and photosensitizer in water were treated as described above for photodecomposition of ABMM. Photooxidation of Trp was studied by exciting the samples at λ_{exc} = 290 nm and following the decrease of the fluorescence intensity at λ = 347 nm. Control experiments showed that under these conditions the fluorescence intensity correlates linearly with Trp concentration. The observed rate constants (k_{obs}) were obtained by a linear least-squares fit of semi-logarithmic plots of ln (I_0/I) *vs.* time.

2.5. Microorganisms and growth conditions

The microorganisms used in this study were the strains of *S. aureus* ATCC 25923, *E. coli* (EC7) and *C. albicans* (PC31), which were previously characterized and identified [22]. Microbial cells were grown aerobically in sterile condition overnight at 37 °C in 4 mL tryptic soy or Sabouraud (Britania, Buenos Aires, Argentina) broths for cultures of bacteria or yeast, respectively. An aliquot (60 μL) of the bacterial culture was aseptically transferred to 4 mL of fresh tryptic soy broth and incubated at 37 °C to exponential phase of growth (absorbance 0.6 at 660 nm). Cells were centrifuged (3000 rpm for 15 min) and re-suspended in equal amount of PBS, corresponding to $\sim 10^8$ colony forming units (CFU)/mL. Then the cells were diluted 1/1000 in PBS, corresponding to $\sim 10^6$ CFU/mL. After overnight cultures of *C. albicans*, cells were harvested by centrifugation (3000 rpm for 15 min) and re-suspended in PBS. Yeast cells (absorbance 0.5 at 650 nm) were diluted 1:4 in PBS to obtain $\sim 10^6$ CFU/mL. After each assay, cell suspensions were serially diluted 10-fold in PBS. From each dilution 20 μL aliquots

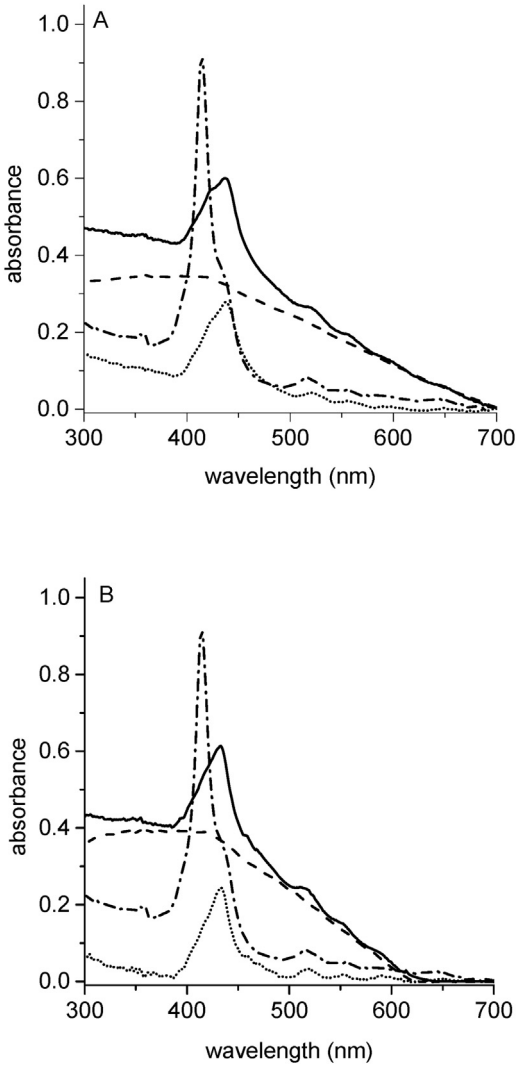

Fig. 3. Absorption spectra of (A) MNPNH-TCPP (solid line), $MNPNH_2$ (dashed line), difference spectrum of MNPNH-TCPP minus $MNPNH_2$ (dotted line) and TCPP (dotted dashed line) in water and (B) MNPSiNH-TCPP (solid line), $MNPSiNH_2$ (dashed line), difference spectrum of MNPSiNH-TCPP minus $MNPSiNH_2$ (dotted line) and TCPP (dotted dashed line) in water.

were streaked horizontally on tryptic soy or Sabouraud agar plates in sextuplicate. Also, cell suspensions were quantified by the spread plate counting method in triplicate for estimating the survival rate of microorganisms. Both techniques showed no significant difference in the results. Viable microbial cells were monitored and the number of CFU was determined after ~24 h (bacteria) or ~48 h (yeast) incubation at 37 °C in the dark.

2.6. Photosensitized inactivation of microorganisms

Cell suspensions of microorganisms (1 mL, $\sim 10^6$ UFC/ml) in PBS were incubated with 0.5 mL stock suspension of nanoparticles in Pyrex culture tubes (13 × 100 mm) for 30 min in dark at 37 °C. This represent the addition of 1.5 mg nanoparticles in a final volume of 1.5 mL that contains 3.0 μM TCPP. Then, 200 μL of each cell suspension were transferred to 96-well microtiter plates (Deltalab, Barcelona, Spain). Cells were exposed for different time intervals (0, 15 and 30 min) to visible light. Viable cells were determined as described above.

2.7. Recycling experiments

Cell suspensions (1 mL, $\sim 10^6$ UFC/ml) were treated with 1.5 mg MNPNH-TCPP or MNPSiNH-TCPP as described above in Section 2.6. Cells were irradiated with visible light for 30 min. After that, MNP were recovered by applying a magnetic field, treated cell suspension was removed and viable cells were determined. Then, a new cell suspension (1 mL, $\sim 10^6$ UFC/ml) was added to MNP, incubated in dark for 30 min and irradiated for 30 min. For each MNP, three cycles of photoinactivation were performed.

2.8. Controls and statistical analysis

Control experiments were performed in presence and absence of photosensitizer in the dark and in the absence of photosensitizer with cells irradiated. The amount of DMF (<1% v/v) used in each experiment was not toxic to microbial cells. Three values were obtained per each condition and each experiment was repeated separately three times. The unpaired *t*-test was used to establish the significance of differences between groups. Differences between means were tested for significance by one-way ANOVA.

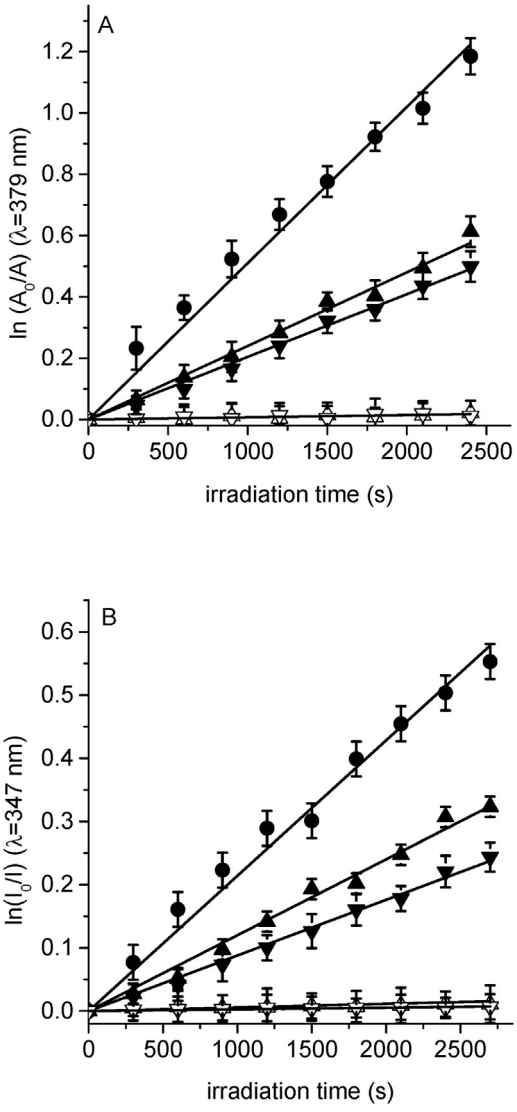

Fig. 4. First-order plots for the photooxidation of (A) ABMM (35 μM) and (B) Trp (20 μM) photosensitized by MNPNH-TCPP (▼), $MNPNH_2$ (▽), MNPSiNH-TCPP (▲), $MNPSiNH_2$ (△) and $TPPS_4^{4-}$ (●) in water, λ_{irr} = 455–800 nm.

Table 1
Kinetic parameters for the photooxidation reaction of ABMM (k_{obs}^{ABMM}) and Trp (k_{obs}^{Trp}) and $O_2(^1\Delta_g)$ quantum yield (Φ_Δ) in water.

Photosensitizer	k_{obs}^{ABMM} (s^{-1})	Φ_Δ	k_{obs}^{Trp} (s^{-1})	$k_{obs}^{Trp}/k_{obs}^{ABMM}$	k_r^{Trp} ($s^{-1}\,M^{-1}$)
MNPNH-TCPP	$(2.04 \pm 0.05) \times 10^{-4}$	0.28 ± 0.03	$(0.87 \pm 0.05) \times 10^{-4}$	0.44	$(4.4 \pm 0.3) \times 10^7$
MNPSiNH-TCPP	$(2.40 \pm 0.06) \times 10^{-4}$	0.33 ± 0.03	$(1.20 \pm 0.05) \times 10^{-4}$	0.50	$(5.0 \pm 0.4) \times 10^7$
$TPPS^{4-}$	$(5.10 \pm 0.08) \times 10^{-4}$	0.71[a]	$(2.14 \pm 0.08) \times 10^{-4}$	0.42	$(4.2 \pm 0.3) \times 10^7$

[a] From Ref. [21].

Results were considered statistically significant with a confidence level of 95% ($p < 0.05$). Data were represented as the mean ± standard deviation of each group.

3. Results and discussion

3.1. Preparation of MNP conjugates

Synthesis of the MNP-porphyrin conjugates were carried out by the reaction between water-resuspended $MNPNH_2$ or $MNPSiNH_2$ and a solution of TCPP activated with EDC and NHS in DMF at 25 °C for 24 h with continuous stirring. The synthetic route to the MNPs conjugated with TCPP is shown in Scheme 1. This is a simplified representation of the processes involved in the synthesis. Carbodiimide activation is a well-established procedure for obtaining amide linkages [15,16]. However, since TCPP has four carboxylic acid groups, it is possible that more than one amide bond to be formed by porphyrin. The conjugates were washed by magnetic decantation with water and ethanol (Fig. 1). Turbid supernatant suggests that there are aggregated nanoparticles in suspension that are not decanted by the magnetic field. This may be due to the formation of small nuclei of nanoparticles and to the decomposition of same magnetite into meghemite in the presence of oxygen [11]. A red coloration was observed in the washes, corresponding to the excess porphyrin. The resulting solids were filtered and washed with the appropriate solvent in order to remove the residual unbound porphyrin. This process was monitored by UV–vis and stopped when no Soret band was detected in the rinse solvent. Nanoparticles were resuspended in 5 mL water to obtain a stock suspension of 3 mg MNPNH-TCPP or MNPSiNH-TCPP/mL. Therefore, the initial amount of nanoparticles did not change in the synthetic process.

TEM images of MNP after different treatments are shown in Fig. 2. A spherical appearance and an average diameter of about 15 nm was found for MNP (Fig. 2A) and $MNPNH_2$ (Fig. 2B). On the other hand, a negligible increase in nanoparticle size was found after being coated with APTS (Fig. 2C). This result coincides with previously published works [23,24]. Moreover, the bonding of TCPP to MNPs did not change the particle size (Fig. 2D). Similar result was previously reported for porphyrins attached to MNP [12]. The images show the formation of aggregates between nanoparticles. This may be due to the attraction between the MNPs for their strong magnetization and the low repulsion generated by the terminal amino groups.

3.2. Determination of the amount of TCPP covalently bound to MNPs

The amino groups attached to the MNP were determined using FDNB. This substrate reacts rapidly with primary amines by a nucleophilic aromatic substitution S_NAr reaction [20]. The excess of FDNB can be quantified by the reaction with *n*-butylamine to form BDNA. Thus, FDNB was reacted with a) MNPSi, b) $MNPSiNH_2$ and c) MNPSiNH-TCPP. From the difference in absorbance ($\Delta A^{350} = 0.100$) between experiments a) and b), 5.7 ± 0.2 nmol NH_2 groups/mg of $MNPSiNH_2$ was calculated. Comparing experiments b) and c) ($\Delta A^{350} = 0.046$), 2.6 ± 0.1 nmol NH_2 groups/mg of MNPSiNH-TCPP was obtained. Therefore, it can be calculated 3.1 ± 0.3 nmol NH_2 groups bonded to TCPP/mg of MNPSiNH-TCPP. Similarly, a value of 2.9 ± 0.3 was obtained for NH_2 groups bonded to TCPP/mg of MNPNH-TCPP.

3.3. UV–visible absorption spectroscopic properties of MNP

The UV–visible absorption spectra of MNPs and TCPP are compared in Fig. 3. Sharp absorption of Soret band was obtained for TCPP, indicating that this photosensitizer is mainly non-aggregated in water. TCPP presented a Soret band at 414 nm and four Q bands at 521, 556, 597 and 651 nm. The molar extinction coefficient at Soret band was determined as $\varepsilon = 3.65 \times 10^5\,M^{-1}\,cm^{-1}$ [25]. The Q band of the free base porphyrin moiety consists of four components: $Q_x(0,0)$, $Q_x(1,0)$, $Q_y(0,0)$ and $Q_y(1,0)$, which are associated with D_{2h} symmetry [26,27]. Spectra of MNPNH-TCPP and MNPSiNH-TCPP were corrected taking into account the absorption of the $MNPNH_2$ and $MNPSiNH_2$, respectively. Suspensions of nanoparticles bearing porphyrin in water showed the typical Soret band at 437 nm for MNPNH-TCPP and 432 nm for MNPSiNH-TCPP. Moreover, it can be observed the Q-bands between 515 and 650 nm of the TCPP attached to the MNP. Thus, the UV–vis spectroscopy results also confirm the binding of TCPP to MNP. In the MNP, the TCPP units showed the Soret and Q bands, similar to the electronic transitions observed for the corresponding tetrapyrrolic macrocycle in solution. However, the bands of TCPP were broader and shifted in comparison with those of monomeric porphyrin in water. The maximum of the Soret band of TCPP showed a ~20 nm bathochromic shift compared to those in solution. These facts indicate the presence of interaction between TCPP in the hyperbranched MNP structure. The red-shift in the UV–vis spectrum from the free porphyrin to the functionalized iron oxide nanoparticles was previously assigned to the formation of a weakly coupled J-aggregate [28]. This effect is also observed in porphyrins immobilized on a surface and may be due to partial aggregation of the photosensitizer [29].

3.4. Photodynamic activity of MNP conjugates

The detection of $O_2(^1\Delta_g)$ in water was carried out using the salt of anthracene derivative ABMM. In the presence of $O_2(^1\Delta_g)$, this molecular probe is converted to the corresponding endoperoxide [30]. The lifetime of $O_2(^1\Delta_g)$ in water is about 4 μs [31]. However, ABMM is an effective acceptor of $O_2(^1\Delta_g)$ because to its high water-solubility [32]. Photooxidation of ABMM induced by these MNP was investigated under aerobic conditions. Also, we compared the results of the MNP with that photosensitized by $TPPS^{4-}$, which was used as a reference. This anionic photosensitizer was chosen to avoid electrostatic interaction with ABMM [14]. Semilogarithmic plots describing the progress of the reaction for ABMM are shown in Fig. 4A. From the first-order kinetic plots, the values of the observed rate constant (k_{obs}^{ABMM}) were calculated. The results are summarized in Table 1. ABMM decomposition was not detected in presence of $MNPNH_2$ or $MNPSiNH_2$ without the TCPP (Fig. 4A). The photodecomposition rate constant of the anthracene derivative mediated by MNPNH-TCPP or MNPSiNH-TCPP was about half of that obtained for $TPPS^{4-}$ in water. The kinetic data of ABMM photooxidation were used to calculate the quantum yield of

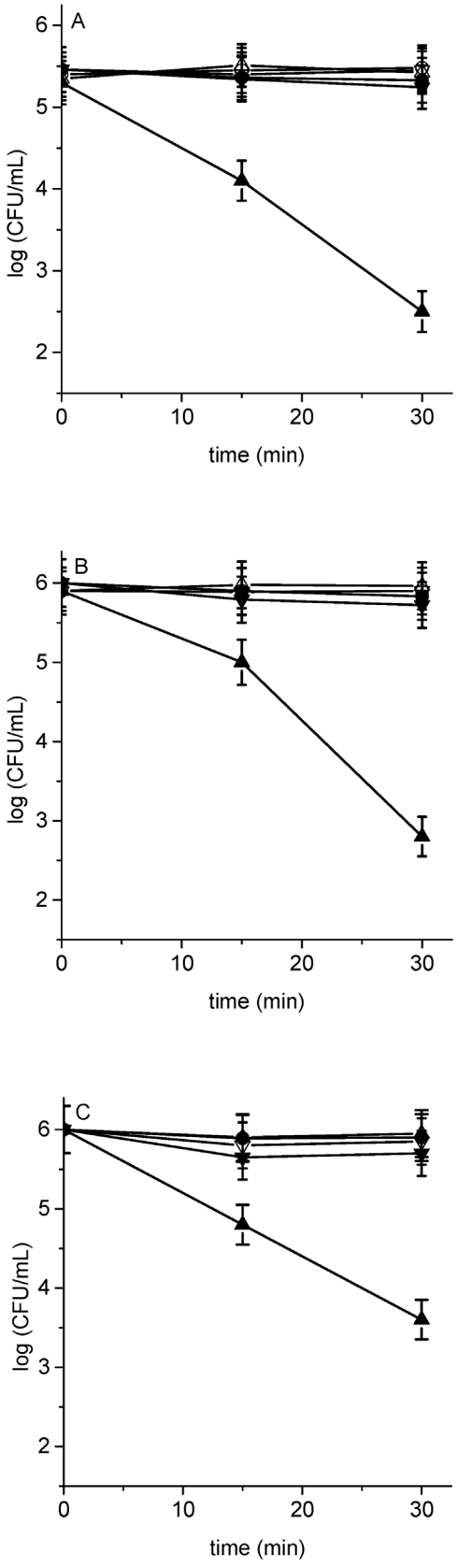

Fig. 5. Survival curves of (A) *S. aureus*, (B) *E. coli* and (C) *C. albicans* cell suspension ($\sim 10^6$ CFU/mL) incubated with $MNPSiNH_2$ (▼) and MNPSiNH-TAPP (▲) for 30 min at 37 °C in dark and irradiated with visible light for different times. Control cultures of cells untreated with the photosensitizer in dark (○) and irradiated (●), cells treated with $MNPSiNH_2$ (▽) and MNPSiNH-TAPP (△) in dark (*$p < 0.05$, compared with control).

$O_2(^1\Delta_g)$ production (Φ_Δ) [14]. The results are shown in Table 1. For both MNP bearing TCPP, the value of Φ_Δ was about 0.3. Thus, the generation of $O_2(^1\Delta_g)$ by these MNP was lower than that of TCPP in water ($\Phi_\Delta = 0.53$) [33]. This is an expected value due to the partial aggregation of TCPP immobilized on MNP. Moreover, the external heavy atom effect of the magnetic nanoparticles could cause a reduction in excited state lifetimes [34]. It was also demonstrated that porphyrin derivatives incorporated onto iron oxide nanoparticles were able to produce $O_2(^1\Delta_g)$ upon irradiation [28]. Therefore, the photodynamic activity sensitized by MNPNH-TCPP or MNPSiNH-TCPP is high enough to induce damage in biological systems.

On the other hand, photooxidation of Trp mediated by MNP was investigated in water. This amino acid can be efficiently photodecomposed by both type I and type II reaction mechanisms [14]. Moreover, Trp can be a potential target of the photodynamic action induced by the MNP. As can be observed in Fig. 4B, the photooxidation of Trp showed first-order kinetics with respect to the amino acid concentration. The values of the k_{obs}^{Trp} for Trp decomposition were calculated from the plots in Fig. 4B. The results are summarized in Table 1. A slightly higher value of Trp reaction rate constant was found using MNPSiNH-TCPP as photosensitizer with respect to MNPNH-TCPP. However, this value is about half of that found for $TPPS^{4-}$ in solution. Also in this case, no photodynamic activity was observed using MNP without TCPP.

From the kinetic results of Trp and ABMM in water under the same experimental conditions, the ratio $k_{obs}^{Trp}/k_{obs}^{ABMM}$ was obtained for MNP bearing TCPP and $TPPS^{4-}$ (Table 1). Similar values were previously obtained for porphyrins as photosensitizers [35,36]. For non-charged porphyrins, the photooxidation of Trp mainly followed a process type II with $k_{obs}^{Trp}/k_{obs}^{DMA}$ values of about 0.4. The reaction rate constant of Trp photooxidation ($k_r^{Trp} = k_r^{ABMM} k_{obs}^{Trp}/k_{obs}^{ABMM}$) [37] was calculated considering a value of $k_r^{ABMM} = 1 \times 10^8\ M^{-1}\ s^{-1}$, similar to that obtained for 9,10-antraceno dipropianato (ADPA) in water [31]. The results are given in Table 1. As can be observed, the values of k_r^{Trp} are very similar to that found for the photooxidation of Trp mediated by $O_2(^1\Delta_g)$ in water ($6.0 \times 10^7\ M^{-1}\ s^{-1}$) [31]. Therefore, these results evidence an important contribution of type II photosensitization in the Trp decomposition induced by MNPNH-TCCP and MNPSiNH-TCCP.

3.5. Photosensitized inactivation of microorganisms

Photoinactivation of *S. aureus*, *E. coli* and *C. albicans* mediated by MNP was investigated in PBS cell suspensions ($\sim 10^6$ CFU/mL) after different periods of irradiations (0, 15 and 30 min) with visible light. Control experiments showed that the viability of microbial cells was unaffected by irradiation alone (Fig. 5). Also, dark incubation with MNP was not toxic to the cells and cell killing was negligible for cells incubated with MNP without porphyrin and irradiated. These controls indicate that the cell mortality obtained after irradiation of the cultures treated with the MNP containing TAPP was is due to the photosensitization effect of the porphyrin, produced by visible light.

Survival curves for cell suspensions treated with MNPSiNH-TCCP are shown in Fig. 5. Photoinactivation of microorganisms was dependent on irradiation times. The photodynamic activity of MNPSiHH-TCCP produced an inactivation of *S. aureus* (Fig. 5A) reaching 3.0 log decrease in cell survival after 30 min irradiation. Similar result was also obtained using MNPNH-TCCP (result not shown). Moreover, *E. coli* cells were inactivated by the photodynamic action of MNPSiHH-TCCP (Fig. 5B). Thus, MNPSiHH-TCCP produced a reduction of 3.1 log in the survival after 30 min irradiation. Under this condition, the photodynamic activity mediated by both MNP containing TCPP was very similar. This reduction represents about 99.9% decrease of cell survival, showing

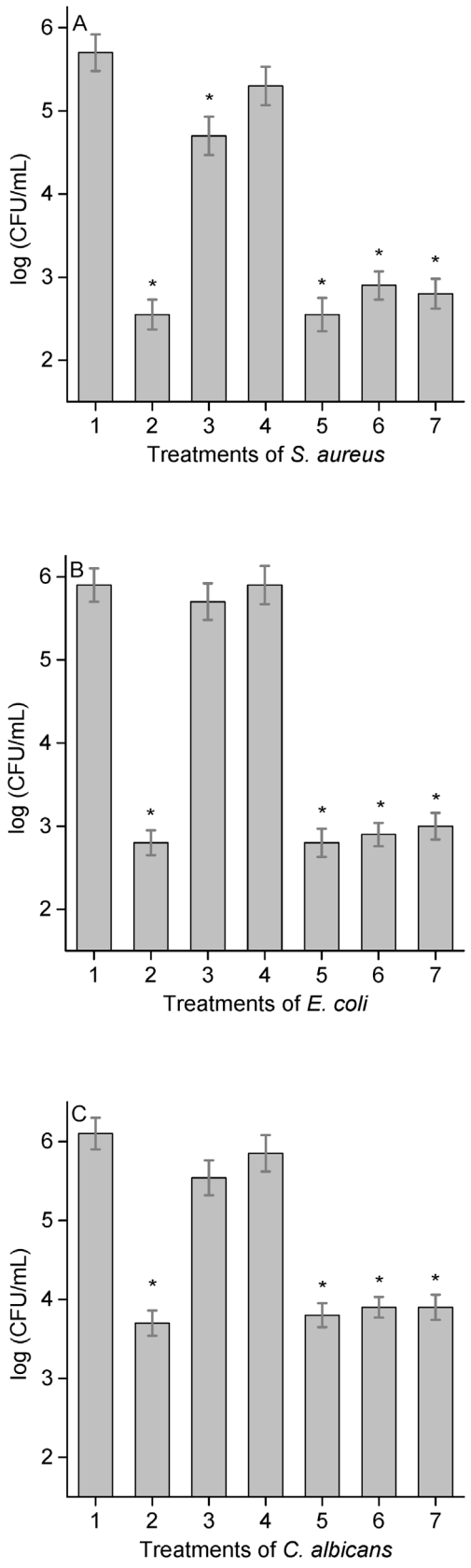

Fig. 6. Survival of (A) *S. aureus*, (B) *E. coli* and (C) *C. albicans* treated with MNP containing TAPP for 30 min at 37 °C in dark and irradiated for 30 min with visible light after different recycling steps; 1) irradiated cells without photosensitizer; 2) 1 st cycle of irradiated cells treated with MNPNH-TAPP; 3) 2nd cycle of irradiated cells treated with MNPNH-TAPP; 4) 3rd cycle of irradiated cells treated with MNPNH-TAPP; 5) 1 st cycle of irradiated cells treated with MNPSiNH-TAPP; 6) 2nd cycle of irradiated cells treated with MNPSiNH-TAPP; 7) 3er cycle of irradiated cells treated with MNPSiNH-TAPP (*$p < 0.05$, compared with control).

that the combination of visible light and TCPP covalently linked to MNP are appropriated photosensitizer to inactivate bacteria. In previous studies, it was demonstrated that cationic nanomagnet-porphyrin hybrids were efficient materials for the photoinactivation of *Enterococcus faecalis*, *E. coli*, and T4-like phage, upon irradiation with white light [12]. Moreover, nanomagnet-porphyrin hybrid with a $CoFe_2O_4$ core showed a remarkable antimicrobial activity by monitoring the bioluminescence of a Gram-negative bacterium (*Allivibrio fischeri*) during the photosensitization process [13].

On the other hand, we investigated the photodynamic activity of MNP to inactivate the yeast *C. albicans*. Fig. 4C shows the survival of *C. albicans* treated with MNPSiHH-TCPP after different irradiation periods. The photodynamic effect yielded a 2.5 log decrease in the cell viability after 30 min irradiation. It was previously established that using cationic porphyrins in solution was possible to obtain an inactivation of >99.99% [22,38]. However, in the present study a 99.7% of cell photoinactivation can be considered appropriated taking into account that the photosensitizer was attached to the MNP. Moreover, the goal of this study is to produce photoinactivation of microbes without contaminating the medium and the possibility of reusing the photosensitizer.

3.6. Recycling of MNP in the PDI of microorganisms

Recycling experiments to photoinactivate *S. aureus*, *E. coli* and *C. albicans* were performed in presence of MNPNH-TCPP and MNPSiNH-TCPP after an irradiation time of 30 min. The results of PDI after each step are shown in Fig. 6. No toxicity was found in the untreated microbial cells after 30 min of irradiation (Fig. 6, line 1). Neither, for the cells incubated with MNPNH-TCPP or MNPSiNH-TCPP after each stage of recycling in the dark (results not shown). For both MNP, the first PDI treatment produced a considerable decrease in cell viability (Fig. 6, lines 2 and 5). A similar photoinactivation capacity was found using MNPNH-TCPP or MNPSiNH-TCPP. However, a considerable decrease in PDI was observed after a second cycle for microorganisms treated with MNPNH-TCPP (Fig. 6, line 3). After a third PDI cycle, photoinactivation of bacteria was negligible using MNPNH-TCPP (Fig. 6B, line 4). Also, survival of *C. albicans* was increased with a third cycle (Fig. 6C, line 4) in presence of MNPNH-TCPP. Thus, efficiency regression with MNPNH-TCPP was more pronounced in the third cycle. The supernatants of the dark controls were translucent, while the supernatants of irradiated samples were brownish (Fig. 7A and B). Also, a decrease in the Soret absorption band was observed in the resuspended MNPNH-TCPP (Fig. 7C). Magnetite (Fe_3O_4) is not very stable and is sensitive to oxidation. Magnetite is transformed into maghemite (γFe_2O_3) in the presence of oxygen [11]. Therefore, the loss of efficiency of the recycling MNPNH-TCPP could be due to oxidation of metal nanomagnetic core after irradiation by $O_2(^1\Delta_g)$ with the consequent demagnetization [12]. This could be possible due to some demagnetization of the magnetic core (Fe^{2+}/Fe^{3+}) of the MNPNH-TCPP during the photodynamic process promoted by the strong oxidizing agent $O_2(^1\Delta_g)$, the main ROS formed during the photodynamic process with this TCPP.

In contrast, after a second cycle of PDI the inactivation of the three microorganisms treated with MNPSiNH-TCPP was the same as in the first treatment (Fig. 6, line 6). Moreover, no changes were observed after a third cycle of PDI (Fig. 6, line 7). Therefore, the silica coating avoids the oxidation, and consequent degradation of

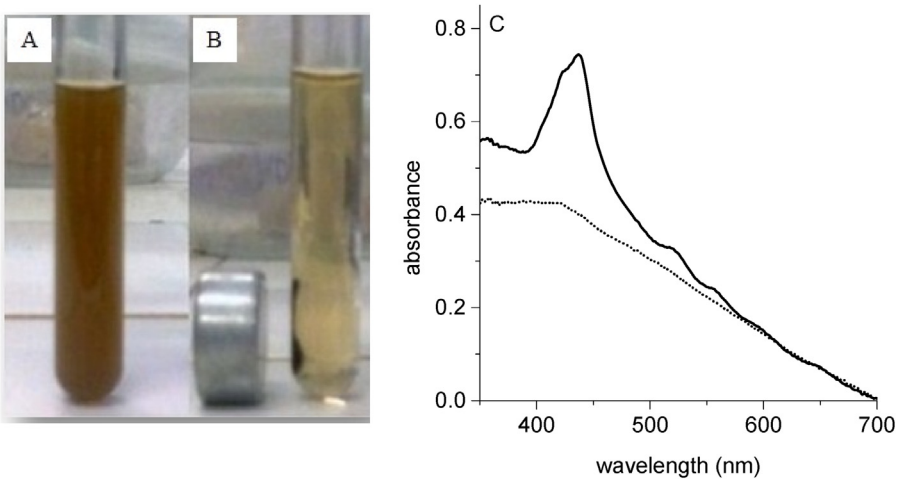

Fig. 7. (A) Suspension of *C. albicans* ($\sim 10^6$ CFU/mL) treated with MNPNH-TCPP and irradiated with visible light for 30 min; (B) after magnetic decantation; (C) absorption spectra of MNPNH-TCPP before irradiation (solid line) and after PDI treatment (dotted line).

the magnetic core. Moreover, this protection given by a silica coating can be also useful to prevent the aggregation and partial decomposition of the naked magnetite [12].

4. Conclusions

In this study, the photodynamic activity of MNPNH-TCPP and MNPSiNH-TCPP was compared in presence of different photooxidizable substrates and in microbial cell suspensions. The mainly difference between these MNP is a silica coating on the surface of MNPSiNH-TCPP. Both particles present a similar size of about 15 nm. UV–visible spectra were mainly characterized by the porphyrin Soret and Q-bands absorptions. In water, these MNP were able to produce $O_2(^1\Delta_g)$ with comparable quantum yields. Moreover, the photodynamic effect of TCPP linked to MNP was effective to sensitize the decomposition of Trp. A type II photoprocess appears to be mainly involved in the photooxidation of this amino acid. PDI *in vitro* studies indicated that MNP containing TCPP are effective photosensitizer to produce photocytotoxic effect in microorganisms. However, the main disadvantage of the MNPNH-TCPP was the lack of stability for recycling PDI treatments. In contrast, repeated PDI treatments can be carried out by recycling MNPSiNA-TCPP in cell suspensions of microorganisms. Therefore, MNPSiNH-TCPP is a promising surface architecture with potential applications in microbial cell photoinactivation. As final remark, this MNPSiNH-TCPP has potential applications as antibacterial materials activated by visible light to control microbial proliferation and maintain aseptic conditions involved in the healthcare. Also, it can be used in the disinfection of microbes in aqueous media. The main advantages of heterogenic eradication of microorganisms using antibacterial MNPSiNH-TCPP are that it can be easily and quickly removed from the media after cell inactivation. This approach avoids permanent photodynamic effects. Also, photosensitizers can be recovered and recycled from the irradiated media, producing minimal environmental pollution.

Acknowledgements

Authors are grateful to Consejo Nacional de Investigaciones Científicas y Técnicas (CONICET, PIP-2015 1122015 0100197 CO) of Argentina, SECYT Universidad Nacional de Río Cuarto (PPI-2016 18/C460) and Agencia Nacional de Promoción Científica y Tecnológica (FONCYT, PICT-2012 0714) of Argentina for financial support. M.G.A. and E.N.D. are Scientific Member of CONICET. A.C.S. and N.S.G. thank to CONICET for the research fellowships.

References

[1] A. Nigama, D. Gupta, A. Sharma, Treatment of infectious disease: beyond antibiotics, Microbiol. Res. 169 (2014) 643–651.
[2] U. Theuretzbacher, Global antibacterial resistance: the never-ending story, J. Glob. Antimicrob. Resist. 1 (2013) 63–69.
[3] G. Criseo, F. Scordino, O. Romeo, Current methods for identifying clinically important cryptic Candida species, J. Microbiol. Methods 111 (2015) 50–56.
[4] D.M.A. Vera, M.H. Haynes, A.R. Ball, T. Dai, C. Astrakas, M.J. Kelso, M.R. Hamblin, G.P. Tegos, Strategies to potentiate antimicrobial photoinactivation by overcoming resistant phenotypes, Photochem. Photobiol. 88 (2012) 499–511.
[5] T.G. St. Denis, T. Dai, L. Izikson, C. Astrakas, R.R. Anderson, M.R. Hamblin, G.P. Tegos, All you need is light: antimicrobial photoinactivation as an evolving and emerging discovery strategy against infectious disease, Virulence 2 (2011) 509–520.
[6] P.R. Ogilby, Singlet oxygen: there is still something new under the sun, and it is better than ever, Photochem. Photobiol. Sci. 9 (2010) 1543–1560.
[7] E. Alves, M.A. Faustino, M.G. Neves, A. Cunha, J. Tome, A. Almeida, An insight on bacterial cellular targets of photodynamic inactivation, Fut. Med. Chem. 6 (2014) 141–164.
[8] C. Spagnul, L.C. Turner, R.W. Boyle, Immobilized photosensitizers for antimicrobial applications, J. Photochem. Photobiol. B: Biol. 150 (2015) 11–30.
[9] S. Noimark, C.W. Dunnill, I.P. Parkin, Shining light on materials – a self-sterilising revolution, Adv. Drug Deliv. Rev. 65 (2013) 570–580.
[10] S. Parveen, R. Misra, S.K. Sahoo, Nanoparticles: a boon to drug delivery, therapeutics, diagnostics and imaging, Nanomed. Nanotech. Biol. Med. 8 (2012) 147–166.
[11] S. Laurent, D. Forge, M. Port, A. Roch, C. Robic, L.V. Elst, R.N. Muller, Magnetic iron oxide nanoparticles: synthesis, stabilization, vectorization, physicochemical characterizations, and biological applications, Chem. Rev. 108 (2008) 2064–2110.
[12] C.M.B. Carvalho, E. Alves, L. Costa, J.P.C. Tomé, M.A.F. Faustino, Neves M.G.P.M.S, A.C. Tomé, J.A.S. Cavaleiro, A. Almeida, A. Cunha, Z. Lin, J. Rocha, Functional cationic nanomagnet-porphyrin hybrids for the photoinactivation of microorganisms, ACS Nano 4 (2010) 7133–7140.
[13] E. Alves, J.M.M. Rodrigues, M.A.F. Faustino, M.G.P.M.S. Neves, J.A.S. Cavaleiro, Z. Lin, Â. Cunha, M. Helena Nadais, J.P.C. Tomé, A. Almeida, A new insight on nanomagneteporphyrin hybrids for photodynamic inactivation of microorganisms, Dyes Pigm. 110 (2014) 80–88.
[14] S.J. Mora, M.E. Milanesio, E.N. Durantini, Spectroscopic and photodynamic properties of 5,10,15,20-tetrakis[4-(3-*N*,*N*-dimethylaminopropoxy)phenyl] porphyrin and its tetracationic derivative in different media, J. Photochem. Photobiol. A: Chem. 270 (2013) 75–84.
[15] Y. Zhang, N. Kohler, M. Zhang, Surface modification of superpramagnetic magnetite nanoparticles and their intracellular uptake, Biomaterials 23 (2002) 1553–1561.
[16] P. Huang, Z. Li, J. Lin, D. Yang, G. Gao, C. Xu, L. Bao, C. Zhang, K. Wang, H. Song, H. Hu, D. Cui, Photosensitizer-conjugated magnetic nanoparticles for *in vivo* simultaneous magnetofluorescent imaging and targeting therapy, Biomaterials 32 (2011) 3447–3458.
[17] M. Mahdavi, M.B. Ahmad, M.J. Haron, Y. Gharayebi, K. Shameli, B. Nadi, Fabrication and characterization of SiO_2/(3-aminopropyl)triethoxysilane-

coated magnetite nanoparticles for lead(II) removal from aqueous solution, J. Inorg. Organomet. Polym. 23 (2013) 599–607.
[18] Z.-Z. Pan, Y.-J. Zhu, Z. Chen, C.-Q. Ruan, L. Xu, Q.-X. Chen, B. Liu, A protein engineering of *Bacillus thuringiensis* δ-endotoxin by conjugating with 4″-O-succinoyl abamectin, Int. J. Biol. Macromol. 62 (2013) 211–216.
[19] I. Halter, Covalently attached organic monolayers on semiconductor surfaces, J. Am. Chem. Soc. 100 (1978) 8050–8055.
[20] N.M. Correa, E.N. Durantini, J.J. Silber, Catalysis in micellar media. Kinetics and mechanism for the reaction of 1-fluoro-2,4-dinitrobenzene with n-butylamine and piperidine in n-hexane and AOT/n-hexane/water reverse micelles, J. Org Chem. 64 (1999) 5757–5763.
[21] V. Gottfried, D. Peled, J.W. Winkelman, S. Kimel, Photosensitizers in organized media: singlet oxygen production and spectral properties, Photochem. Photobiol. 48 (1988) 157–163.
[22] D.D. Ferreyra, E. Reynoso, P. Cordero, M.B. Spesia, M.G. Alvarez, M.E. Milanesio, E.N. Durantini, Synthesis and properties of 5,10,15,20-tetrakis[4-(3-*N*,*N*-dimethylaminopropoxy)phenyl]chlorin as potential broad-spectrum antimicrobial photosensitizers, J. Photochem. Photobiol. B: Biol. 158 (2016) 243–251.
[23] S.S. Banerjee, D.-H. Chen, Fast removal of copper ions by gum arabic modified magnetic nano-adsorbent, J. Hazard. Mater. 147 (2007) 792–799.
[24] M.-H. Liao, D.-H. Chen, Preparation and characterization of novel magnetic nano-adsorbent, J. Mater. Chem. 12 (2002) 3648–3659.
[25] D. Praseuth, A. Gaudemer, J.-B. Verlhac, I. Kraljic, I. Sissoëff, E. Guillé, Photocleavage of DNA in the presence of synthetic water-soluble porphyrins, Photochem. Photobiol. 44 (1986) 717–724.
[26] R.V. Maximiano, E. Piovesan, S.C. Zílio, A.E.H. Machado, R. de Paula, J.A.S. Cavaleiro, I.E. Borissevitch, A.S. Ito, P.J. Gonçalves, N.M. Barbosa Neto, J. Photochem. Photobiol. A: Chem. 214 (2010) 115–120.
[27] J.S. Baskin, H.-Z. Yu, A.H. Zewail, Ultrafast dynamics of porphyrins in the condensed phase: I. Free base tetraphenylporphyrin, J. Phys. Chem. A 106 (2002) 9837–9844.
[28] O. Penon, M.J. Marín, D.B. Amabilino, D.A. Russell, L. Pérez-García, Iron oxide nanoparticles functionalized with novel hydrophobic and hydrophilic porphyrins as potential agents for photodynamic therapy, J. Colloid Interface Sci. 462 (2016) 154–165.
[29] M.B. Ballatore, J. Durantini, N.S. Gsponer, M.B. Suarez, M. Gervaldo, L. Otero, M. B. Spesia, M.E. Milanesio, E.N. Durantini, Photodynamic inactivation of bacteria using novel electrogenerated porphyrin-fullerene C_{60} polymeric films, Environ. Sci. Technol. 49 (2015) 7456–7463.
[30] K.I. Setsukinai, Y. Urano, K. Kakinuma, H.J. Majima, T. Nagano, Development of novel fluorescence probes that can reliably detect reactive oxygen species and distinguish specific species, J. Biol. Chem. 278 (2003) 3170–3175.
[31] F. Wilkinson, W.P. Helman, A.B. Ross, Rate constants for the decay and reactions of the lowest electronically excited singlet state of molecular oxygen in solution. An expanded and revised compilation, J. Phys. Chem. Ref. Data 24 (1995) 663–1021.
[32] M. Wang, S. Maragani, L. Huang, S. Jeon, T. Canteenwala, M.R. Hamblin, L.Y. Chiang, Synthesis of decacationic [60] fullerene decaiodides giving photoinduced production of superoxide radicals and effective PDT-mediation on antimicrobial photoinactivation, Eur. J. Med. Chem. 63 (2013) 170–184.
[33] C.R. Lambert, E. Reddi, J.D. Spikes, M.A.J. Rodgers, G. Jori, The effects of porphyrin structure and aggregation state on photosensitized processes in aqueous and micellar media, Photochem. Photobiol. 44 (1986) 595–601.
[34] H. Ali, J.E. van Lier, Metal complexes as photo- and radiosensitizers, Chem. Rev. 99 (1999) 2379–2450.
[35] M.E. Milanesio, M.G. Alvarez, J.J. Silber, V. Rivarola, E.N. Durantini, Photodynamic activity of monocationic and non-charged methoxyphenyl porphyrin derivatives in homogeneous and biological medium, Photochem. Photobiol. Sci. 2 (2003) 926–933.
[36] M.E. Milanesio, M.G. Alvarez, V. Rivarola, J.J. Silber, E.N. Durantini, Porphyrin-fullerene C_{60} dyads with high ability to form photoinduced charge-separated state as novel sensitizers for photodynamic therapy, Photochem. Photobiol. 81 (2005) 891–897.
[37] T.C. Tempesti, J.C. Stockert, E.N. Durantini, Photosensitization ability of a water soluble zinc(II)tetramethyltetrapyridinoporphyrazinium salt in aqueous solution and biomimetic reverse micelles medium, J. Phys. Chem. B 112 (2008) 15701–15707.
[38] E.D. Quiroga, S.J. Mora, M.G. Alvarez, E.N. Durantini, Photodynamic inactivation of Candida albicans by a tetracationictentacle porphyrin and its analogue without intrinsic charges inpresence of fluconazole, Photodiagn. Photodyn. Ther. 13 (2016) 334–340.